ELSEVIER

Fusion Engineering and Design 28 (1995) 769–775

Fusion Engineering and Design

# Integral test of Kerma data for SS-304 stainless steel in the D–T fusion neutron environment

Y. Ikeda [a], A. Kumar [b], K. Kosako [a], C. Konno [a], Y. Oyama [a], F. Maekawa [a], M.Z. Youssef [b], M.A. Abdou [b], H. Maekawa [a]

[a] *Department of Reactor Engineering, Japan Atomic Energy Research Institute, Tokai, Ibaraki 319-11, Japan*
[b] *School of Engineering and Applied Science, University of California, Los Angeles (UCLA), Los Angeles, CA 90024, USA*

**Abstract**

An experiment to determine nuclear heating rates in an SS-304 assembly was conducted using the intense D–T neutron source FNS at JAERI, within the framework of the JAERI–USDOE collaborative program on fusion neutronics. The distribution of the heat deposition rate at a depth of up to 200 mm in an SS-304 assembly was measured directly with a microcalorimeter incorporated within the intense D–T neutron source. A heat transfer calculation code ADINAT, coupled with the neutron and $\gamma$-ray transport DOT3.5, was applied to derive a time dependence temperature profile in SS-304 probes during irradiation. It was demonstrated that the ADINAT is a powerful tool for analyzing the nuclear heating process in materials with low thermal conductivity such as SS-304. The measured heating rates were compared with comprehensive calculations to verify the adequacy of the currently available database relevant to the nuclear heating process. The analysis based on JENDL-3 nuclear data demonstrated that the calculation of heat deposition on SS-304, in general, was in good agreement with measurements.

## 1. Introduction

The importance of nuclear heating in structural materials has been recognized from the point of view of system design of D–T fusion reactors. Requirements for a reduction in design margin are addressed stringently from critical design criteria. The uncertainty of the database for nuclear heating is considered one of the most crucial problems for the development of first-wall–blanket–shield designs for ITER. Many data libraries have been compiled and issued to be implemented in the neutron transport code system [1–6]. The adequacy of these data, however, has not been tested owing to lack of suitable experimental data.

In order to provide substantial experimental data for data testing, nuclear heating experiment in an SS-304 assembly was carried out at the fusion neutronics source (FNS) [7] at the Japan Atomic Energy Research Institute (JAERI) within the framework of the JAERI/USDOE collaborative program on fusion neutronics. The present experiment was an extension of previous single probe experiments [8–10]. The data in this experimental configuration, however, were expected to be more suitable for validation of calculations of the neutron spectrum where the D–T neutron contribution is less important and associated $\gamma$-ray and slow neutron contributions are dominant. As the SS-304 is a relatively low thermal conductivity material, the time de-

Elsevier Science S.A.
*SSDI* 0920-3796(94)00325-4

pendent temperature change due to heat flow in the probe material was analyzed with the heat transfer analysis code ADINAT [11]. The measured temperature rise due to nuclear heating was corrected by the ADINAT analysis. Measured data at depths up to 200 mm in the SS-304 assembly were compared with the DOT3.5 [12] calculation using KERMA data based on the JENDL-3 nuclear data file [13]. The ratios of calculated to experimental results (C/E) are discussed with emphasis on the adequacy of the JENDL-3 nuclear database.

## 2. Experiment

### 2.1. System configuration

Fig. 1 illustrates the cross-section of the assembly consisting of an SS-304 core region, side $Li_2CO_3$ enclosure and polyethylene insulator. The outer regions of the side with respect to the $d^+$ beam direction were covered with $Li_2CO_3$ bricks. The supporting frame used in phase II series experiments of the JAERI/USDOE collaboration [8–10] was utilized. The front surface was placed close to the D–T neutron source in order to maximize the neutron flux levels inside the SS-304 core, resulting in a high signal to noise (S/N) ratio. As shown, the D–T neutron source was not enclosed with the materials. Thus, a large amount of slow neutrons reflected off the wall of the target room were expected to impinge on the assembly from the front and rear surfaces. From the side, the influence of the slow neutrons returned by the room was mitigated by the $Li_2CO_3$ and polyethylene layers. The nominal size of the SS-304 core was $357 \times 458 \times 458\ mm^3$. Cubicle blocks of SS-304 with unit dimensions $51 \times 51 \times 51\ mm^3$ were contained in the SS-304 stainless steel box and stacked along the central axis of the assembly.

Based on previous experience of limits of detector sensitivity due to background noise of the system, the test region was enclosed in an SS-304 box to ensure an air-tight system. The idea of applying the SS-304 block

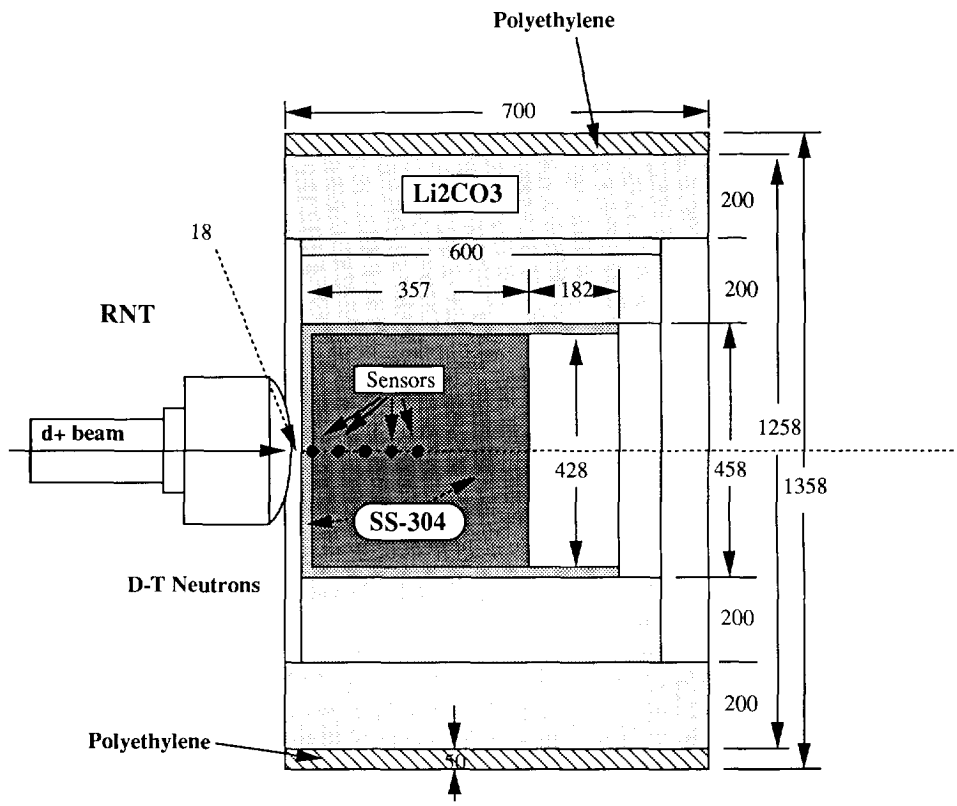


Fig. 1. Cross-sectional view of the SS-304 assembly. The dimensions are given in millimeters.

itself as probe material was based on the assumption that heat flow is not significant in the short period during the sampling times, e.g. 30–100 s, when a thermal insulator is attached on each block. On the surface closer to the D–T neutron source, TM (10 kΩ) sensors were attached and thin leading wires were extracted through the thin space between blocks. On the side of the last block at a depth range 170–220 mm, a 100 Ω RTD was attached and also extracted utilizing a small space between blocks. The extracted wires were connected directly to Keithly-181, 182, 182 and Solatron-7081 voltmeters. The data acquisition scheme was the same as for previous single probe experiments [8–10].

### 2.2. Experimental measurement

Sampling times of 30–120 s, longer than the 10 s used for the single probe measurements, were applied to increase the effective temperature rise. If adiabatic conditions are assumed, we can have a larger accumulation of heat deposition, resulting in a higher temperature rise. In order to observe a slight change at deep positions, this scheme was essential. However, another uncertainty was introduced in the determination of the realistic temperature due to heat flow in the relatively large probe zone and to the relatively large gradient of the heating rate. However, we chose this scheme knowing these drawbacks.

The D–T neutron source strength of $(2–3) \times 10^{12}$ s$^{-1}$ was almost identical with that of previous experiments with the single probe configuration. The same long pulsed neutron operation was applied to discriminate between the background drift produced by slow components due to radiation, heat conduction through both cable lines and paper insulators attached to adjacent SS-304 blocks. In addition, self-heating by resistance of the thermal sensor should be factored into the slow component. For the same reason as given for the long sampling time, neutron pulse lengths of 5–10 min were applied. The data acquisition diagram is shown in Fig. 2.

## 3. Experimental results

The derivatives of temperature changes for the SS-304 block detectors are shown in Fig. 3. The data at the position closest to the D–T neutron source display the highest values with strong overshoots and undershoots at the beginning and end of the neutron pulse irradiation respectively. This profile is very similar to that observed in an $Li_2CO_3$ probe in the previous experiments. Considering the relatively low thermal conductivity of SS-304 and the steep gradient of the neutron flux over the large block detector 51 mm in length, the variation in the derivatives during irradiation is explained by heat transfer from the front to rear sides. This effect due to heat flow was also observed in the data from the second position. The neutron flux gradient at this position was expected to be much smaller

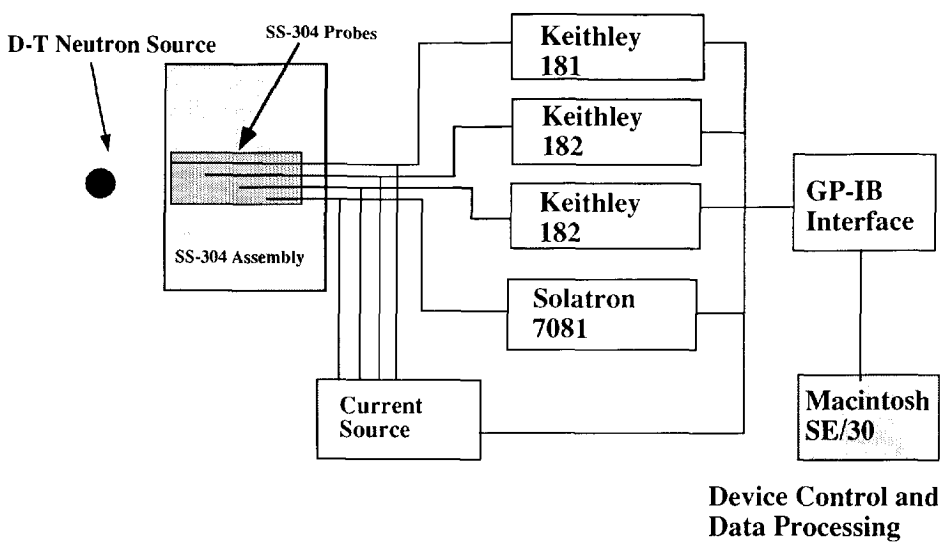


Fig. 2. Block diagram of direct nuclear heating measurements with a microcalorimeter.

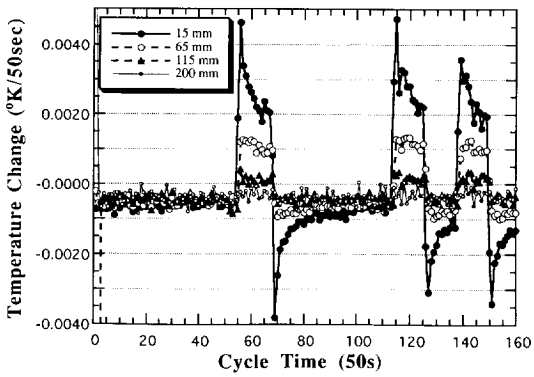


Fig. 3. Rate of temperature change in the SS-304 probes due to D–T neutron irradiation.

than that at the first probe. At the third position, an almost flat distribution was detected. Although the data at the last position at a depth of 210 mm measured with the RTD are identical with the background drift line, there is a slight rise on average. Throughout these SS-304 assembly experiments, a longer cycle time of 50 s was adopted to increase the temperature rise, assuming adiabatic conditions within the probe. The temperature rise due to nuclear heating was derived from the first rise in the rate of temperature change. Fig. 4 shows a plot of all measured data. The temperature rise decreases with depth in the SS-304. This trend is reasonable given the steep neutron flux distribution. The rate of temperature change with a drastic decrease at the first probe shown in Fig. 3, however, suggested that there was strong heat flow within the first 50 s, although the thermal conductivity of SS-304 is low.

Table 1
Physical properties and dimensions of the SS-304 probe

| Item | Value |
|---|---|
| Dimension (mm) | $51 \times 51 \times 51$ |
| Density (g mm$^{-3}$) | $7.82 \times 10^{-4}$ |
| Thermal conductivity (W mm$^{-1}$ K$^{-1}$) | $16.3 \times 10^{-2}$ |
| Specific heat (J mm$^{3}$ K$^{-1}$) | $4.286 \times 10^{-5}$ |
| Boltzmann constant (J K$^{-1}$) | $0.1380658 \times 10^{-22}$ |
| Radiation coefficient | $0.39 \times 10^{-1}$ |

In order to estimate the temperature change over a duration of 50 s, the heat transport code ADINAT was applied. The ADINAT code treated all possible heat transfer phenomena in terms of heat conduction, convection and radiation. All the conditions and data used are given in Table 1. The heat source distribution was determined from neutron and $\gamma$-ray fluxes calculated by DOT3.5 with the FUSION-J3 cross-section library based on JENDL-3. The experimental analysis is given in the next section in detail. Simulating the probe configuration, the time-dependent temperature change was calculated with the DOT3.5/ADINAT coupled code for the position of the front surface of the first SS-304 block probe. The difference in temperature change at the first sampling time point with different sampling times is shown in Fig. 5. As shown, at first the temperature rise is less as the sampling time increases. It is naturally understood that if the neutron flux is constant, the nuclear heating rate is also constant. However, the heat flow toward the deeper region, where the

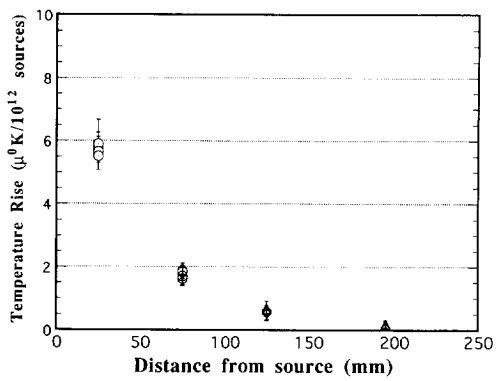


Fig. 4. Measured temperature rise distribution. The values are normalized with respect to the D–T neutron source strength of $10^{12}$ n s$^{-1}$.

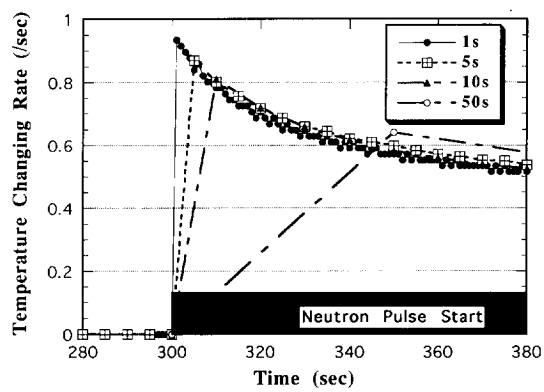


Fig. 5. Difference in temperature change at the first sampling time point with different sampling times.

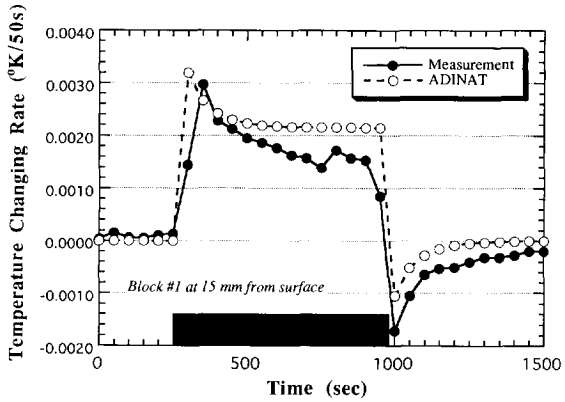


Fig. 6. Comparison of calculations by ADINAT with measurement.

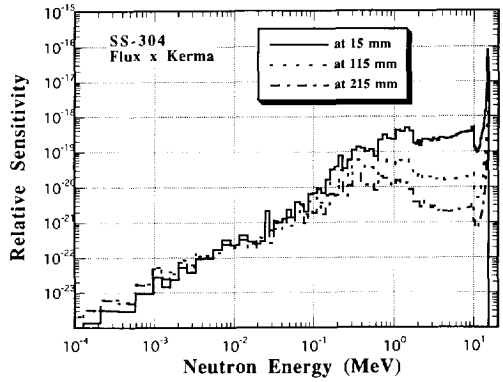


Fig. 7. Differential sensitivities of the neutron heating rate for SS-304 at 15, 115 and 215 mm from the surface of the SS-304 assembly.

lower temperature rise is associated with a low nuclear heating rate, was negative at the front surface of the probe. As time passed, the rate of temperature change decreased and stabilized at equilibrium. A correction factor for data with 50 s sampling time was derived assuming that data with 1 s sampling time give a realistic temperature rise without heat flow. The experimental data to be analyzed were obtained by correcting the measured data shown in Fig. 4 with derived factors at all positions. A direct comparison of ADINAT calculation with measurement is shown in Fig. 6. The comparison demonstrates that the heat transport analysis was appropriate for investigation of the time-dependent temperature change.

## 4. Analysis

Experimental analysis was carried out to examine the adequacy of the current data relevant to nuclear heating. Neutron and $\gamma$-ray fluxes were calculated using the two-dimensional transport code DOT3.5 and FUSION-J3 cross-section library based on JENDL-3. The experimental system was modeled as an $R-Z$ cylindrical geometry and the $P_5$-$S_{16}$ approximation was applied. The neutron Kerma data were created from FUSION-J3 [14] by a direct method, counting all contributing reaction cross-sections. The Kerma for $\gamma$-rays was derived from DLC-99 [15]. Calculated differential sensitivities of neutron Kerma multiplied with neutron spectra are shown in Fig. 7. The D–T neutron peak fraction decreases with depth appreciably, whereas the fraction of low energy components does not decrease so rapidly. In particular, the flux in the energy region below 100 keV does not change according to the position. Moreover, the neutron flux below 10 keV, in contrast, increases as the depth increases. The fraction of 14 MeV at 215 mm becomes only 2% of the total neutron flux. Thus, the nuclear heating rate at this position is contributed to mainly by low energy neutrons. This indicates that the present neutron flux spectrum is suitable in terms of integral testing of the heating rate for a wide energy range and overall validation of the calculation.

## 5. Discussion

The experimental data before and after correction for heat flow are plotted in Fig. 8 along with the calculated

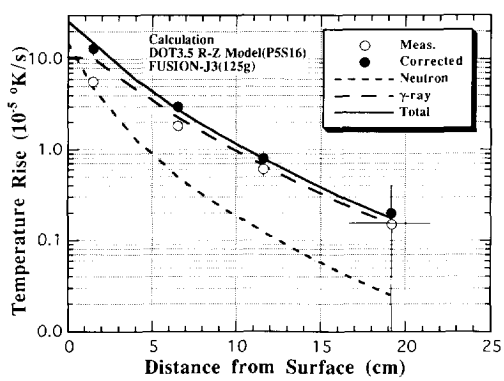


Fig. 8. Measured and calculated nuclear heating distributions in the SS-304 assembly.

data. The neutron and $\gamma$-ray fractional contributions are given separately in addition to the total heating rate. The results clearly demonstrate that consideration of the heat transfer is essential for determining the heating rate when a large size detector is used. The general agreement between the calculation and experiment suggests that the nuclear data for SS-304 employed in this analysis are adequate as long as the validity of the correction method is assured.

Kerma factors of $\gamma$-rays also have an ascending profile for almost all materials at an energy higher than several hundred kiloelectron volts. At lower energy below 100 keV, kerma of $\gamma$-rays increases greatly. However, the spectrum is dominated by $\gamma$-rays with energy ranging from hundreds of kiloelectron volts to 10 MeV. Emphasis should be placed on this as, from Fig. 8, the $\gamma$-ray contribution to the heating rate becomes more dominant as the depth of the position increases.

The neutron and $\gamma$-ray spectra at deeper positions of the shielding structure are very similar to those at 215 mm in the present assembly. It is worthwhile noting that these experimental data are assumed be appropriate for verification of the data and method to be applied in design calculation.

The present study shows the possibility of applying the calorimetric method for measurement of the total nuclear heating, for validating the design calculation. However, uncertainty in the nuclear heating at deeper regions, e.g. at the interface between the shield structure and following insulator and superconducting magnet, depends on the uncertainty in calculation of the neutron and $\gamma$-ray flux spectra. In order to arrive at sufficient levels of uncertainty for design calculation, the neutron and $\gamma$-ray flux spectra should be determined. More effort is to be directed toward a dosimetry study.

## 6. Conclusion

The SS-304 assembly experiment provided nuclear heating distribution data at depths up to 200 mm. It was suggested that a stronger neutron source and more sensitive thermal detection system are required to measure the data in deeper regions. However, regarding simulation of the neutron spectrum for the field of interest in shield design for a fusion reactor, this type of integral experiment is very effective for validation of the overall nuclear heating process. Although further examination of the data is needed to reduce the uncertainty, the present results demonstrate that calculations based on JENDL-3 are fairly adequate within experimental error. In conclusion, the experimental approach with a microcalorimeter demonstrated in the present study offers a promising way to obtain experimental data for validating the adequacy of design calculations and associated nuclear data.

## Acknowledgments

The authors would like to express their sincere thanks to J. Kusano, C. Kutsukake, S. Tanaka and Y. Abe for operation of the FNS accelerator in the particular experimental request. Dr. T. Nakamura is thanked for his valuable advice and encouragement for the experimental program in the earlier stage. The US contribution was supported by USDOE.

## References

[1] M.A. Abdou, C.W. Maynard and R.W. Wright, MACK: a computer program to calculate neutron energy release parameters (fluence-to-kerma factor) and multigroup reaction cross sections from nuclear data in ENDF format, ORNL-TM-3994, July 1973 (Oak Ridge National Laboratory, Oak Ridge, TN).

[2] M.A. Abdou and C.W. Maynard, Calculation method for nuclear heating– part I: theoretical and computational algorithms, Nucl. Sci. Eng., 56 (1975) 360.

[3] M.A. Abdou and C.W. Maynard, Calculation methods for nuclear heating– part II: application to fusion reactor blanket and shields, Nucl. Sci. Eng., 56 (1975) 381.

[4] Y. Farawila, Y. Gohar and C.W. Maynard, KAOS/LIB-V: a library of nuclear response functions generated by KAOS-V code from ENDF/B-V and other data files, ANL/FPP/TM-241, 1989.

[5] K. Maki, H. Kawasaki, K. Kosako and Y. Seki, Nuclear heating constant KERMA library, JAERI-M 91-073, 1991 (Japan Atomic Energy Research Institute, Ibaraki) (in Japanese).

[6] M. Kawai, S. Iijima, T. Aruga, T. Fukahori, K. Maki, K. Shibata, T. Sugi, Y. Yamanouti, K. Kitao, A. Takahashi and N. Yamano, Review of the research and application of KERMA factor and DPA cross section, JAERI-M 91-043, 1991 (Japan Atomic Energy Research Institute, Ibaraki) (in Japanese).

[7] T. Nakamura, H. Maekawa, J. Kusano, Y. Oyama, Y. Ikeda, C. Kutsukake, S. Tanaka and S. Tanaka, Present status of the fusion neutron source (FNS), Proc. 4th Symp. on Acceleratora Science and Technology, RIKEN, Saitama, 24–26 November 1982, 155–156.

[8] A. Kumar, Y. Ikeda and C. Konno, Experimental measurements and analysis of nuclear heat deposition rates in simulated D–T neutron environment: JAERI/USDOE collaborative program on fusion neutronics experiments, Fusion Technol., 19 (1991) 1979.

[9] A. Kumar, M.Z. Youseff, M.A. Abdou, Y. Ikeda, C. Konno, K. Kosako, Y. Oyama and T. Nakamura, Direct nuclear heating measurement in fusion neutron environment and analysis, Fusion Eng. Des., 18 (1991) 397–405.
[10] Y. Ikeda, C. Konno, K. Kosako, Y. Oyama, F. Maekawa, H. Maekawa, A. Kumar, M.Z. Youseff and M.A. Abdou, Measurement and analysis for nuclear heat depositions in structural materials induced by D–T neutrons, Fusion Technol., 21 (1992) 2190.
[11] ADINAT, A Finite Element Program for Automatic Dynamic Incremental Nonlinear Analysis of Temperature, ADINA Engineering, Inc., 1984.
[12] W.A. Rhoades and F.R. Mynatt, The DOT III two-dimensional discrete ordinates transport code, ORNL/TM-4280, 1979 (Oak Ridge National Laboratory, Oak Ridge, TN).
[13] K. Maki, K. Kosako, Y. Seki and H. Kawasaki, Nuclear group constant set FUSION-J3 for fusion reactor nuclear calculations based on JENDL-3, JAERI-M 91-072, (Japan Atomic Energy Research Institute, Ibaraki).
[14] K. Shibata, T. Nakagawa, T. Asami, T. Fukahori, T. Narita, S. Chiba, M. Mizumoto, A. Hasegawa, Y. Kikuchi, Y. Nakajima and S. Igarasi, Japanese evaluated nuclear data library, Version-3, JAERI-1319, 1990 (Japan Atomic Energy Research Institute, Ibaraki).
[15] R.W. Roussin, J.R. Knight, J.H. Hubbell and R.J. Howerton, Description of DLC-99/HUGO package of photon interaction data in ENDF/B-V format, ORNL/RSIC-46 (ENDF-335), 1983 (Oak Ridge National Laboratory, Oak Ridge, TN).